International Journal of Mass Spectrometry 310 (2012) 1–9

Contents lists available at SciVerse ScienceDirect

International Journal of Mass Spectrometry

journal homepage: www.elsevier.com/locate/ijms

On quantitative measurements of peroxycarboxylic nitric anhydride mixing ratios by thermal dissociation chemical ionization mass spectrometry

Levi H. Mielke[1], Hans D. Osthoff*

University of Calgary, Department of Chemistry, Calgary, AB T2N 1N4, Canada

ARTICLE INFO

Article history:
Received 10 August 2011
Received in revised form 21 October 2011
Accepted 25 October 2011
Available online 30 October 2011

Keywords:
Peroxycarboxylic nitric anhydrides (PAN)
Thermal dissociation chemical ionization mass spectrometry (TD-CIMS)
Interferences
Quantitative measurements

ABSTRACT

Thermal dissociation chemical ionization mass spectrometry (TD-CIMS) has become an increasingly popular tool for rapid and sensitive quantification of peroxycarboxylic nitric anhydrides (PANs), which are important trace gas constituents of the troposphere. In TD-CIMS, the PANs are thermally dissociated in a heated inlet to NO_2 and peroxyacyl radicals, which are converted in electron transfer reactions with iodide reagent ions to the corresponding carboxylate anions. Here, we evaluate the performance of the TD-CIMS method in the presence of interferences that occur in polluted air masses. Response factors of the TD-CIMS were determined using laboratory-generated air samples and parallel measurements of NO_2 and ΣPAN by blue diode laser thermal dissociation cavity ring-down spectroscopy (TD-CRDS) and of NO_y by NO-O_3 chemiluminescence (CL). The TD-CIMS was less sensitive to peroxymethacryloyl nitric anhydride (MPAN) than to other PANs tested, which was rationalized by differences in the temperature dependent loss rates of the peroxyacyl radicals in the heated inlet. To track matrix effects, photochemically generated ^{13}C-labeled PAN was continuously added as an internal standard. The presence of NO or NO_2 in the sample gas mixture resulted in signal suppression, which could be corrected using the internal standard. The presence of organic acids resulted in a redistribution of count intensity between carboxylate anions, impacting the instrument's ability to accurately quantify PANs other than peroxyacetic nitric anhydride under moderately polluted conditions.

1. Introduction

Peroxycarboxylic nitric anhydrides (PANs, general structure $RC(O)O_2NO_2$, where R is typically an alkyl group) have long been recognized as important trace gas constituents of the troposphere (e.g., [1–4]). Commonly referred to by their non-IUPAC name peroxyacyl nitrates, the PANs are known as lachrymators and are phytotoxic to plants at high concentration [5]. The PANs are formed in the same photochemistry between NO_x ($\equiv NO + NO_2$) and volatile organic compounds (VOCs) that produces ozone (O_3); thus, the relative PAN abundances contain information on the VOCs involved in the ozone-formation. For example, peroxypropanoic nitric anhydride (PPN, $C_2H_5C(O)O_2NO_2$) is a tracer of anthropogenic VOCs that react to form propanal, whereas peroxymethacryloyl nitric anhydride (MPAN, $H_2C{=}C(CH_3)C(O)O_2NO_2$), produced by abstraction of the aldehydic hydrogen in methacrolein [6], is a tracer of isoprene oxidation chemistry [7,8]. PANs are susceptible to thermal dissociation, but are quite stable in the mid and upper troposphere as the rates of thermal dissociation, photolysis and OH-initiated degradation reactions are slow [9]. As a consequence, PANs can act as NO_x reservoir species and be transported over long distances, slowly releasing NO_x in the form of NO_2 and affecting ozone production in many regions of the troposphere [10–15]. Of the more than 43 different PANs that have been detected in ambient air so far, peroxyacetic nitric anhydride (usually called peroxyacetyl nitrate or PAN, $CH_3C(O)O_2NO_2$) is the most abundant PAN species and often also the most abundant odd nitrogen, or NO_y ($\equiv NO_x + \Sigma PANs + \Sigma RONO_2 + HNO_3 + NO_3 + 2N_2O_5 + HONO + ClNO_2 + \ldots$), species, in particular in the mid to upper troposphere [16].

The most commonly used technique to quantify PANs in ambient air has been gas chromatography with electron capture detection (GC-ECD). In state-of-the-art GC-ECD instruments, run times of less than one minute and limits of detection of a few parts-per trillion by volume (pptv, 10^{-12}, v/v) have been achieved [17]. However, ECD detectors are prone to interference from halogenated species and oxygen and exhibit different response factors for different PANs. Alternatively, PANs have been detected post-column by thermal dissociation (TD) to, and quantification of, NO_2 by luminol chemiluminescence (CL) [18] or luminol CL coupled to peroxy radical chemical amplification [19]:

$$RC(O)O_2NO_2 \xrightarrow{\Delta} RC(O)O_2 + NO_2 \quad (1)$$

* Corresponding author. Tel.: +1 403 220 8689.
E-mail address: hosthoff@ucalgary.ca (H.D. Osthoff).
[1] Now at: School of Public and Environmental Affairs, Indiana University, Bloomington, IN 47405, United States.

1387-3806/$ – see front matter © 2011 Elsevier B.V. All rights reserved.
doi:10.1016/j.ijms.2011.10.005

In a variant of the TD technique, the time-consuming separation step is bypassed, and the PANs are quantified as ΣPAN by selective TD and detection (of the generated NO_2) using laser-induced fluorescence (TD-LIF) [20,21] or cavity ring-down spectroscopy (TD-CRDS) [22,23].

In recent years, mass spectrometric techniques to quantify mixing ratio of PANs in ambient air have become popular, offering the advantages of fast measurement speeds, high sensitivity, and high selectivity. For example, mixing ratios of PAN, PPN and MPAN have been quantified by proton transfer reaction mass spectrometry (PTR-MS) utilizing H_3O^+ reagent ion with limits of detection of <70 pptv (15 s) [24]. However, detection of PAN using its protonated organic peroxy product ion at m/z 77 ($CH_3C(O)OOHH^+$) suffers from interference by acetone–water clusters and protonated peracetic acid [25]. More recently, selected ion flow tube mass spectrometry (SIFT-MS) using H_3O^+ reagent ion has been used to quantify PAN at m/z 122 ($CH_3C(O)OONO_2H^+$) with limits of detection of 20 pptv (10 s) [26].

An alternative mass spectrometric method that has been gaining in popularity is iodide ion thermal dissociation chemical ionization mass spectrometry (TD-CIMS) [27–33]. In iodide ion TD-CIMS, the PANs are dissociated in a heated inlet via reaction (1), and the generated peroxyacyl (PA) radicals react with I^- to form the corresponding carboxylate anions:

$$RC(O)O_2 + I^- \xrightarrow{H_2O} RCO_2{}^- + IO \quad (2)$$

The carboxylate anions are usually mass-selected using a quadrupole mass filter, but an ion trap has also been recently used [32]. The detection limits (<10 pptv) and response times (<1 s) of iodide ion TD-CIMS instruments are superb – even allowing for measurements of PAN deposition rates by eddy covariance [30,33]. However, the TD-CIMS response factors vary between PAN species [31,34]. Further, interference from NO_2, NO and other peroxy radicals which remove peroxy radicals generated in the heated inlet must be considered.

$$RC(O)O_2 + NO_2 \rightarrow RC(O)O_2NO_2 \quad (-1)$$

$$RC(O)O_2 + NO \rightarrow RC(O)O + NO_2 \xrightarrow{O_2} RO_2 + CO_2 + NO_2 \quad (3)$$

$$RC(O)O_2 + R'O_2 \rightarrow \text{products} \quad (4)$$

Usually, an isotopically labeled PAN ($^{13}CH_3{}^{13}C(O)O_2NO_2$, hereafter referred to as ^{13}C-PAN) is added to the TD-CIMS inlet as an internal standard [17,31].

An added complication is that carboxylate anions proton-exchange with acids, for example carboxylic acids:

$$RCO_2^- + R'CO_2H \rightarrow RCO_2H + R'CO_2^- \quad (5)$$

Reaction (5) has recently been utilized to monitor organic and inorganic acids with acetate reagent ion [35,36]. Furthermore, iodide ion TD-CIMS suffers from interference from peroxycarboxylic acids [34]:

$$RC(O)O_2H + I^- \rightarrow RCO_2^- + HOI \quad (6)$$

The peroxycarboxylic acids are usually less abundant than PANs in ambient air [37] but can nevertheless be a significant interference, for example in photochemical PAN sources [34].

Our research group has recently acquired a commercial TD-CIMS and has described its design and application (with iodide reagent ion) to measurement of nitryl chloride ($ClNO_2$) [38]. In this paper, we focus on the application of iodide ion TD-CIMS to measurements of PAN abundances in ambient air. We investigated why TD-CIMS is considerably less sensitive to MPAN compared to PAN and PPN [27]. Matrix effects and the response to interferences (including NO, NO_2, and organic acids) were characterized using laboratory-generated air samples containing PAN, PPN, or MPAN and parallel measurements of NO_2 and ΣPAN by blue diode laser TD-CRDS and of NO_y by NO–O_3 CL. To track matrix effects, the TD-CIMS was equipped with a photochemical source of ^{13}C-PAN as internal standard. Advantages and limitations of applying iodide ion TD-CIMS to measure PAN abundances and challenges associated with measurements of less abundant PANs in ambient air are discussed.

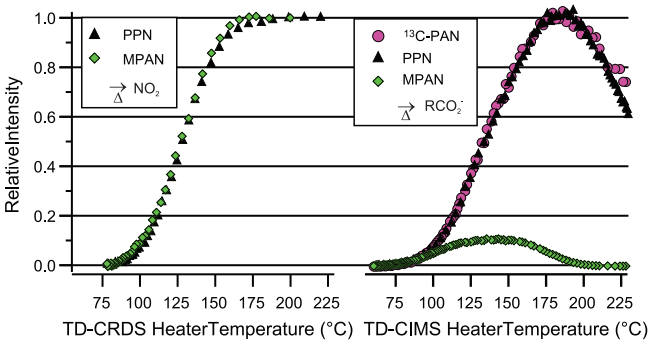

Fig. 1. Thermal dissociation profiles for PPN and MPAN using TD-CRDS (left-hand side) and for ^{13}C-PAN, PPN, and MPAN using the TD-CIMS (right-hand side). The yield of NO_2 exhibits the same temperature dependence for PPN and MPAN, whereas the yield of methacrylate is considerably different from that of ^{13}C acetate or propionate.

2. Experimental

2.1. Chemical ionization mass spectrometry of peroxycarboxylic nitric anhydrides

The CIMS was purchased from THS Instruments (Atlanta, GA) and is a compact version of the one described by Slusher et al. [27]. A schematic of the instrument is shown in Fig. 1 of Mielke et al. [38]. Briefly, the CIMS is comprised of three differentially pumped regions that house an ion-molecule reaction chamber (IMR) operated at 21 Torr, a collisional dissociation chamber (CDC) to break up water clusters which is evacuated by a molecular drag pump (Alcatel MDP 3011) to a pressure of 0.5 Torr, an octopole ion guide ($\sim 10^{-3}$ Torr), and a 3/4 in. quadrupole mass analyzer ($<10^{-5}$ Torr) with channeltron detector (Ceramax 7550M). The ion guide and mass analyzer regions are evacuated by a pair of 250 L/s turbo pumps (Varian, model Turbo-V 81-M). Sample gas entered the CIMS via a pinhole and was diluted with a flow of 400 standard cubic centimeters per minute (sccm) of humidified nitrogen to ensure that formation of carboxylate anions via reaction (2) was independent of the humidity of the sample air [38]. Iodide reagent ions were generated by passing 1 sccm of 150 parts-per-billion by volume (ppbv) CH_3I in N_2 diluted with a flow of 1.2 standard-liters per minute (slpm) of N_2 gas past a ^{210}Po radioactive ion source (NRD P-2031, 20 mCi activity) and were added to the IMR via a side arm. The mass analyzer is controlled using a modified RF unit (Extrel U72) and was operated in selective ion mode. A typical list of masses monitored and dwell times are given in Table S1 of [38]. Mass counts were normalized to 10^6 counts of I^- before presentation.

For the experiments in this manuscript, the CIMS sampled from an inlet constructed from 1/2 in. outer diameter (o.d.) and 3/8 in. inner diameter (i.d.) FEP Teflon tubing. Approximately 50 sccm of ^{13}C-PAN internal standard (approximate mixing ratio 7.5 ppbv) were added to the sampled air via a PFA Teflon Tee. The ^{13}C-PAN was generated photochemically using the source described in [34] and was monitored at m/z 61. A 11.5 cm section of the inlet was heated to (typically) 180–190 °C to dissociate the PANs to PA radicals and NO_2 as per reaction (1). This heated section of the TD inlet could be bypassed with a 3-way valve, if desired, and was followed by a 14 cm long section of unheated Teflon tubing. One end of this

tubing was notched and pressed gently against the front plate of the CIMS which contained a pinhole. The Teflon tubing was cut in such a way as to not generate a tight seal and to allow air escape to the sides. The instrument drew a total sample flow of approximately 3.0 slpm of which 1.32 slpm were sampled into the CIMS via the pinhole, with the remaining 1.68 slpm pumped to exhaust. The function of this bypass flow was to reduce inlet residence times and to minimize the impact of reactions ((−1) and (3)–(4)). The total volume of the inlet and the inlet flow rate is similar to those used in other TD-CIMS instruments (e.g., [27,28,31,32]).

2.2. Measurements of NO_2 and ΣPAN by blue diode laser cavity ring-down spectroscopy

The TD-CRDS has been described in detail elsewhere [23]. Briefly, the instrument uses two optical detection cells: one serves as a reference channel and is used to monitor (background) NO_2 mixing ratios, and the other utilizes a heated inlet consisting of a 1/4 in. outer diameter (o.d.) quartz tube heated to 250 °C to quantitatively dissociate PANs to NO_2 via reaction (1). Mixing ratios of NO_2, and NO_2 plus NO_2 generated from PAN thermal dissociation, are monitored by absorption at 405 nm. Mixing ratios of ΣPANs are quantified by calculating difference between the sample and reference channels. The TD-CRDS suffers from a negative interference in the presence of NO_2 due to reaction (−1) and from a positive interference in the presence of NO. Mixing ratios of ΣPAN reported by TD-CRDS were corrected for both interferences as described by Paul and Osthoff [23].

2.3. Chemiluminescence measurements of NO and NO_y

Mixing ratios of NO and NO_y were monitored using a commercial NO_y chemiluminescence (CL) analyzer (Thermo Scientific, Model 42iTL). This instrument utilizes a molybdenum converter heated to 325 °C to convert the various NO_y species to NO, which is quantified by NO-O_3 CL. An automated valve is used to switch between NO_y and (background) NO. The manufacturer-specified detection limit of the CL analyzer is 50 pptv over a 120 s averaging time. Corrections of the NO/NO_y data due to varying concentrations of water vapor (which affects the sensitivity of the CL measurement) were not necessary, since a common source of zero air was used as make-up gas in all experiments.

The calibration of the NO/NO_y CL instrument was periodically verified using an NO/N_2 calibration standard (Praxair, 2.8 or 99.5 parts-per-million (10^{-6}, ppmv), certified) and an NO_2/air standard (Praxair, 120 ppmv, certified). The output of these cylinders was diluted with zero air, with the flows set by mass flow controllers. The amount of NO_2 delivered was verified by simultaneous CRDS measurements.

2.4. Synthesis and delivery of standards and TD-CIMS calibration

PAN, PPN, and MPAN were synthesized following procedures by J. Roberts [personal communication], which are based on the methods by Nielsen and Gaffney [39,40]. Briefly, PAN, PPN, and MPAN were synthesized from the corresponding peroxycarboxylic acids, generated by reaction of H_2O_2 with acetic or propionic anhydride, respectively. The peroxycarboxylic acids were then reacted with a mixture of HNO_3 and H_2SO_4 at 0 °C. Small aliquots were stored in tridecane in a freezer until use.

Dilute gas mixtures of PAN, PPN, or MPAN were generated using a capillary diffusion source stored in an ice/water bath whose output was diluted in ultra-pure ("zero") air (ZA, Praxair). Typically, ~60 sccm of N_2 or ZA were passed over the diffusion source and diluted with up to 12 slpm of ZA. This large flow was needed to provide sufficient sample volume to enable parallel measurements by TD-CIMS, TD-CRDS, and NO/NO_y CL. Response factors of the TD-CIMS for PAN, PPN, and MPAN were determined against parallel measurements of the diffusion source output by TD-CRDS. In some experiments (see below) the photochemical source described by Furgeson et al. [34] was used to deliver a stable gas stream of PAN.

2.5. Interference tests with laboratory-generated samples

In the first set of experiments, variable amounts of NO or NO_2, delivered from reference gas cylinders (Praxair) via mass flow controllers, were added to the output of the PAN, PPN, or MPAN diffusion sources. In a second set of experiment, formic or propanoic acid vapor, delivered using a temperature controlled permeation source (VICI "Dynacalibrator" Model 120 with permeation tubes supplied by Kintek), were added to a dilute gas stream of PAN generated using the photochemical source. The concentrations of NO and NO_2 in the sample stream were quantified by CRDS and NO CL, whereas the concentrations of the acids were calculated using flow dilution and the manufacturer-specified permeation rates.

2.6. Test measurements of PANs in ambient air

Test measurements of ambient air were conducted at a local rooftop site [38] in February, 2011 and during Calnex-LA in Pasadena, CA, from May to June, 2010 (CIMS only). At the rooftop site, the CIMS, CRDS, and CL instruments sampled from a common inlet manifold. Automated valves were used to regularly bypass the internal standard, to overflow the inlet with zero air (or N_2), or to add a small stream of excess NO (Praxair, 0.1% in N_2).

3. Results

3.1. Optimization of inlet temperature and TD-CIMS calibration

Fig. 1 shows relative responses of the TD-CRDS and TD-CIMS to laboratory-generated samples containing MPAN or PPN as a function of the instruments' inlet temperatures. The NO_2 yield curve from TD of PPN (observed by TD-CRDS) as a function of temperature is the same as that of MPAN. The yields of the corresponding peroxyacyl radicals (observed as carboxylate anions by TD-CIMS), on the other hand, are quite different. Whereas PPN (observed as propionate at m/z 73) and ^{13}C-PAN (internal standard, observed as ^{13}C-acetate at m/z 61) exhibit a similar response with a maximum signal at an inlet temperature of 180 °C, considerable less signal is observed for MPAN (observed as methacrylate at m/z 85). Further, the maximum response for MPAN is at an inlet temperature of 140 °C. The observed TD profiles were not significantly affected by concentration changes between experiments.

Based on data shown in Fig. 1, we chose an inlet temperature of 190 °C as our "standard" operating temperature of the TD-CIMS inlet. Table 1 summarizes the TD-CIMS response factors measured under these conditions. The response factors for PAN and PPN were approximately equal (~18 counts/pptv), whereas the MPAN response factor was only 0.4 counts/pptv; thus, the relative response of MPAN and PAN in our TD-CIMS was approximately 1:44.

3.2. Correction of matrix effects due to NO_2 and NO using ^{13}C-PAN internal standard

Fig. 2 shows a time series of simultaneous measurements of PPN in zero air, to which various amounts of NO_2 were added. The TD-CRDS monitored NO_2 (green color, top panel) and ΣPAN (shown in red, bottom panel). The TD-CRDS data were corrected using Eq. (7b) in [22] before presentation; the correction was too small in magnitude to be visible on the scale of this graph. The TD-CIMS response

Table 1
Typical response factors and limit of detection (LOD) of the TD-CIMS for PANs.

Acronym	IUPAC name	Detected at m/z	Sensitivity (counts/s/pptv)	Standard deviation of the background (1σ) (counts/s)	LOD (3σ) (pptv)
PAN	Peroxyacetic nitric anhydride	59	17.8[a]	15.9	2.7
PPN	Peroxypropionic nitric anhydride	73	17.8	8.9	1.5
MPAN	Peroxymethacroyl nitric anhydride	85	0.4	17.2	130

[a] Same as PPN [34].

at m/z 73 (propionate anion) and the response at m/z 61 (internal standard) are shown in black and purple, respectively (middle panel). Clearly, both traces are affected by the presence of NO_2 due to reaction (−1) in the CIMS inlet. At 15:47, only PPN was added to the inlet; because its thermal dissociation generates NO_2, the addition of PPN suppresses the counts at m/z 61 by approximately 800 counts. The black trace (bottom panel) shows the apparent response of the TD-CIMS, calculated from the counts at m/z 73 multiplied by the inverse of the TD-CIMS response factor determined in the previous section. Shown as a blue trace are the mixing ratios of PPN corrected for CIMS matrix effects, calculated from:

$$[\mathrm{PPN}]_{\mathrm{corrected}} = (\mathrm{PPN\ response\ factor}) \times (m/z\,73_{\mathrm{obs}}) \times \frac{m/z\,61_{\mathrm{blank}}}{m/z\,61_{\mathrm{obs}}}. \quad (7)$$

In Eq. (7), $m/z\,61_{\mathrm{blank}}$ are counts observed at m/z 61 during times when the CIMS only sampled zero air and the internal standard (i.e., prior to 15:46 and after 16:27 in Fig. 1), interpolated to the times when PPN was added. Following this correction, the TD-CRDS and TD-CIMS mixing ratios are well correlated, and independent of added NO_2.

The use of Eq. (7) assumes that there are negligible background counts at m/z 61 in the absence of the internal standard, that the signal at m/z 61 is derived from reactions of ^{13}C-PAN, that contributions from ^{13}C-labeled acetic or peroxyacetic acid co-emitted by the photochemical source are negligible, and that there are negligible background counts at m/z 73. While this was the case for the data shown in Fig. 2, these assumptions may not be valid for ambient air data. In practice, the relevant "background" counts can be determined by regularly bypassing the internal standard and by addition of excess NO to the inlet and subtracting the observed counts from those used in Eq. (7).

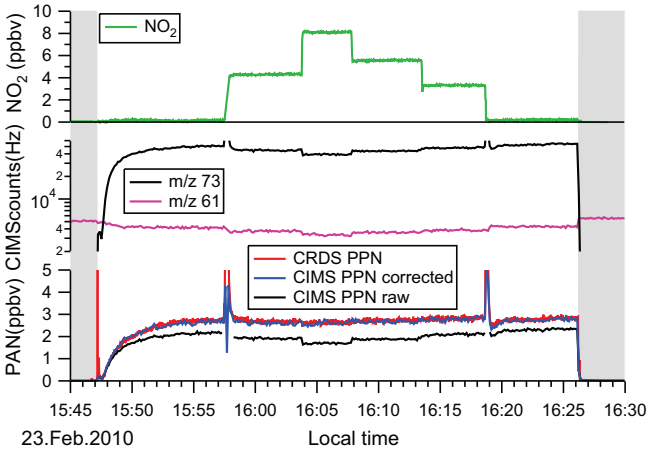

Fig. 2. Simultaneous measurements of PPN and NO_2 mixtures by TD-CRDS and TD-CIMS. (top panel) Mixing ratios of NO_2 added and quantified by CRDS (middle panel). Ion counts observed at m/z 73 (propionate from PPN) and m/z 61 (^{13}C-acetate from ^{13}C-PAN). Both exhibit a negative interference to NO_2 due to recombination of the thermal dissociation products. (bottom panel) Mixing ratios of PPN observed by TD-CRDS and by TD-CIMS, before and after correcting the signal for matrix effects. Both instruments report PPN mixing ratios in quantitative agreement with each other.

Fig. 3 demonstrates how the TD-CIMS and TD-CRDS measurements of PPN in zero air are affected by the addition of NO. The NO mixing ratios, monitored by CL, are shown as the purple-colored trace alongside NO_2 monitored by CRDS (top). The TD-CIMS signal at m/z 73 (black trace, middle panel) is suppressed due to reaction (3) occurring in its inlet, which is mirrored by the internal standard (m/z 61, shown in purple). The TD-CRDS signal is amplified by the added NO (not shown). Correction of the raw TD-CRDS data using Eq. (9) in [23] and TD-CIMS data using Eq. (7) yield PPN mixing ratios that are in excellent numerical agreement with each other (bottom panel): the slope of the scatter plot (not shown) is 1.008 ± 0.003 ($r^2 = 0.95$; intercept forced to zero). These results show that matrix effects arising from the presence of NO or NO_2 in ambient air can be corrected for using the internal standard.

Fig. 4 shows a comparison of the matrix effects arising from the presence of either NO or NO_2. At 5 pbbv of added NO_x, for example, the PPN signal is suppressed by 50% in case of NO and 20% in case of NO_2. The pseudo-first order rate constant for the signal suppression is approximately 4 times that in the presence of NO compared to in the presence of an equimolar amount of NO_2. This ratio is about twice that determined by Sehested et al. [41] for the reaction of peroxacetyl radical with NO and NO_2 and suggests that reaction (−1) between the peroxyacyl radical and NO_2 is reversible in the CIMS inlet.

3.3. Matrix effects due to organic acids

3.3.1. Effect of internal standard

Panel A of Fig. 5 shows an experiment in which the CIMS inlet was flooded with N_2 containing variable mixing ratios of formic

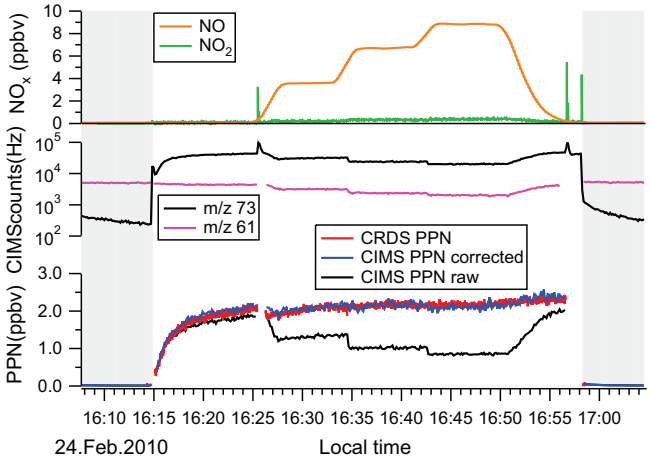

Fig. 3. Simultaneous measurements of PPN and NO mixtures by TD-CRDS and TD-CIMS. (Top panel) Mixing ratios of NO and NO_2, quantified by NO-O_3 chemiluminescence and CRDS, respectively. (Middle panel). Ion counts observed at m/z 73 (propionate from PPN) and m/z 61 (^{13}C-acetate from ^{13}C-PAN), which both exhibit a negative interference due to titration of the PP and ^{13}C-PA radicals by NO. (Bottom panel) Mixing ratios of PPN observed by TD-CRDS and by TD-CIMS, before and after correcting the signal for matrix effects The TD-CRDS signal has been corrected for its amplification by NO [23] before presentation. Both instruments report PPN mixing ratios in quantitative agreement with each other.

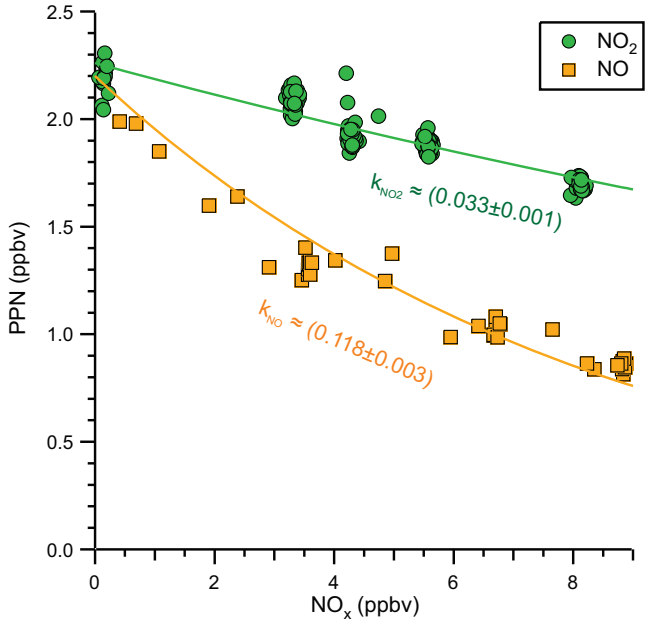

Fig. 4. Plots of the CIMS PPN signal (in ppbv) as a function of NO_2 and NO mixing ratios added. The lines are pseudo-first order exponential fits with the decay constant as indicated on the graph.

acid (HCOOH). Concentrations of HCOOH were gradually changed from 3 to 750 ppbv (top axis) by increasing the oven temperature of the permeation source. Addition of HCOOH results in suppression of counts at m/z 61 (derived from ^{13}C-PAN internal standard), consistent with proton exchange (reaction (5)) of HCOOH with ^{13}C-labeled acetate anion generated from PAN and ^{13}C-PAN and subsequent reaction with I^- (reactions (1) and (2)). The solid green line shows counts m/z 61 when the HCOOH source was taken offline to verify the stability of the internal standard. When the internal standard was taken offline, there were very few counts at m/z 45 observed (green squares), verifying that counts at m/z 45 arise from proton exchange with acetate ions (as opposed to I^- chemistry).

Panel A of Fig. S-1 shows the same experiment as in panel A of Fig. 5, but with propionic acid (mixing ratios from 3 to 750 ppbv) instead of formic acid. The same result as before was obtained: propionic acid proton-exchanges with ^{13}C-labeled acetate to yield m/z 73, and very little response is observed in the absence of the internal standard.

Thus, the addition of ^{13}C-PAN internal standard results in "false" signals at other masses. For the examples shown in panel A of Figs. 5 and S-1, addition of ~8 ppbv of HCCOH produced ~200 counts/s at m/z 45 (Fig. 5), and addition of ~8 ppbv of propanoic acid produced ~73 counts/s at m/z 73 (~4 pptv of "fake PPN", Fig. S-1). Both artifacts are negligibly small.

3.3.2. *Effect of PAN*

Panel B of Fig. 5 shows the same experiment as in panel A, but with approximately 2.2 ppbv of PAN (m/z 59) added from a photochemical source. Again, addition of HCOOH results in suppression of acetate ion counts at m/z 59 and m/z 61, consistent with proton exchange. The top trace in panel C shows a time series of m/z 59 when the HCOOH source was taken offline (blue circles) and the m/z 59 signal corrected using the response of the internal standard, i.e., the right-hand side term in Eq. (7). Both methods give consistent (approximately 40,000) counts at m/z 59 throughout this experiment. This shows that matrix effects arising from the addition of an organic acid at m/z 59 can be corrected with an internal standard, but that a non-PAN derived signal is observed at the mass corresponding to the acid (m/z 45 in this case).

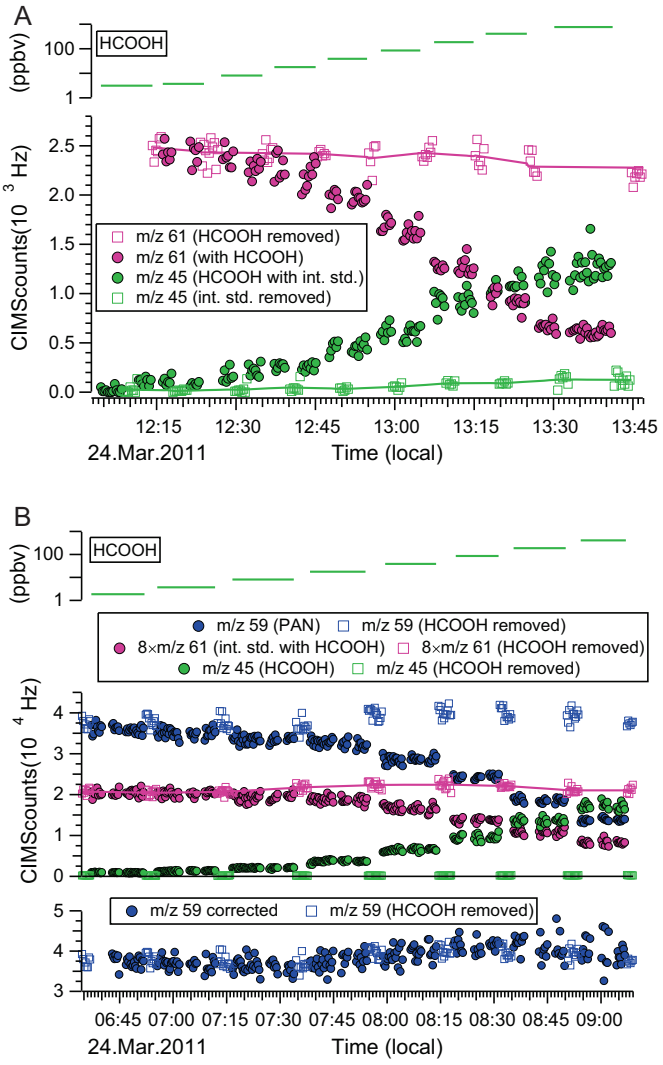

Fig. 5. Characterization of proton exchange reactions. Panel A: proton exchange with 100 pptv of ^{13}C-PAN with formic acid. (Top panel) Approximate mixing ratio of formic acid delivered from the permeation source. (Bottom panel) CIMS ion counts observed at m/z 61 (^{13}C-acetate) and m/z 45 (formate). The circles show data points collected when both the ^{13}C-PAN photo source and the formic acid source were sampled. The squares show data points collected when either the photo source (int. std.) or the acid source was momentarily bypassed. Very few counts at m/z 45 are observed in the absence of ^{13}C-PAN. (Panel B) Similar experiment as in panel A, but with a constant amount of approximately 2.2 ppbv of PAN (monitored at m/z 59) added to the gas sample stream. (Top panel) Approximate mixing ratio of formic acid. (Middle panel) CIMS counts at m/z 59, 61, and 45, showing proton-exchange between acetate and formate. The formate signal generated is considerably larger than in panel A, in spite of similar formic acid concentrations delivered, but due to greater abundance of acetate reagent ion. (Bottom panel) Comparison of m/z 59 counts during times when the formic acid source was bypassed with m/z 59 corrected using the internal standard.

Panel B of Fig. S-1 shows the same experiment as in panel A of Fig. 5, but with propionic acid instead of formic acid. The same result as before was obtained: propionic acid proton-exchanges with acetate and ^{13}C-labeled acetate. Thus, the presence of PAN results in "false" signals at other masses. For the examples shown in Panels B of Figs. 5 and S-1, addition of ~8 ppbv of HCCOH produced ~2000 counts/s at m/z 45 (Fig. 5), and addition of 8 ppbv of propanoic acid produced 1000 counts/s at m/z 73 (56 pptv of "fake PPN", Fig. S-1).

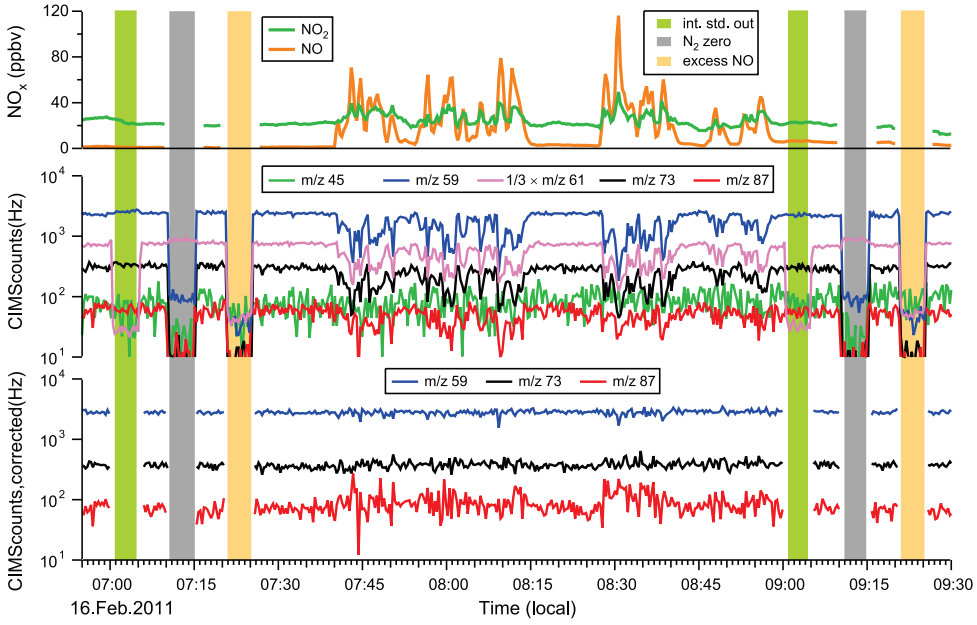

Fig. 6. Performance of the internal standard correction under ambient conditions. (Top panel) Mixing ratios of NO and NO_2 observed by CL and CRDS. (Middle panel) Raw CIMS signal at m/z 45, 59, 61 (internal standard, divided by 3), 73, and 87. All masses associated with known PANs (except m/z 45) are inversely correlated with NO_x. (Bottom panel) Mass counts corrected for matrix effects using the internal standard.

3.4. Measurements of PANs in ambient air

Fig. 6 shows a time series of ambient air data collected in Calgary. At this particular location and time, photochemical production and thermal dissociation of PANs in ambient air was rather slow; hence, the mixing ratios of PANs were approximately constant and change mainly during air mass shifts. The period shown in Fig. 6 was chosen as the air was contaminated by emissions from an idling tour bus parked at a nearby building. The top panel shows measurements of NO and NO_2. NO mixing ratios peaked at above 100 ppbv. The second panel shows the "raw" CIMS counts at m/z 45, 59, 61, 73, and 87 (n- and i-butanoate, derived from peroxybutanoic nitric anhydride). The latter four masses are clearly anticorrelated with those of the NO and NO_2, whereas the counts at m/z 45 are unaffected by NO_x. Corrections of the raw counts at m/z 59, 61, 73, and 87 using Eq. (7) produce nearly "flat" signals (bottom panel). There is some residual structure remaining, most visible in the m/z 59 time series, which arises because the CIMS is operated in selective ion mode and the measurements at m/z 59 and m/z 61 are not simultaneous. By and large, the internal standard allows for an accurate correction of the PAN, PPN, and PBN signals for matrix effects arising from NO and NO_2.

When the internal standard is removed, counts at m/z 61 drop from about 2400 to a background level of ~90 counts/s in both instances shown (as green underlay). In the first instance, the number of counts at m/z 59 slightly increases. This implies that the internal standard slightly suppresses formation of acetate anion. We speculate that this is because of NO_2 co-eluted by the photochemical source, which removes peroxyacyl radical via reaction (−1). When the inlet is flooded with N_2 (gray underlay), most counts drop to baseline levels, except for the internal standard (which increases) and m/z 59. The latter is slightly elevated because of (slow) desorption of PANs from the inner walls of the inlet and because the isotopically labeled standard is not 100% pure. When excess NO is added (purple underlay), all masses associated with PANs are titrated to background levels.

There is a reduction in the counts at m/z 45 when the inlet is flooded with N_2 and, to a lesser extent, when excess NO is added, which suggests that carboxylate anions (generated from PANs) participate in the conversion of formic acid to formate anion in the IMR. At the same time, the counts at m/z 45 are not affected by ambient NO_x levels, which suggests that formic acid is likely the limiting reagent and that a rather modest amount of acetate anion suffices to produce a signal at m/z 45 in this case.

Fig. 7 shows a CIMS inlet temperature scan conducted during Calnex-LA, where the abundances of PANs and organic acids were considerable compared to Calgary. The top panel shows raw counts observed at mass counts associated with known PANs expected to present in the sample air at m/z 59 (PAN), 71 (acrylic nitric anhydride, $H_2C{=}C(O)O_2NO_2$, APAN), 73 (PPN), 87 (PiBN), and 121 (peroxybenzoic nitric anhydride, $C_6H_5CO_2NO_2$, PBzN), mass counts associated with the ^{13}C-PAN internal standard at m/z 61, and mass counts associated with PANs which are not expected to be abundant in ambient air at m/z 45 (peroxyformic nitric anhydride, HCO_2NO_2, PFN), 75 ($HOCH_2CO_2NO_2$, HPAN) and 89 (peroxyoxalic nitric anhydride, $HCO_2CO_2NO_2$, PON) [16]. The counts observed at an inlet temperature of 60 °C relative to those at 180 °C were highly variable, depending on the ion monitored (top panel, Fig. 7). In some cases, e.g., m/z 45 and 61, the background was elevated due to very high counts at m/z 46 (NO_2^-) and m/z 62 (NO_3^-), which partially contributed to mass counts at adjacent masses in this campaign. The bottom panel shows the normalized and background-subtracted relative responses. All masses exhibit the same temperature dependence. This implies that proton exchange with acetate ions (generated from TD of PAN and subsequent reaction of PA radical with I^-) was the main ionization mechanism. In particular, counts at m/z 45, 75, and 89 arise from proton-exchange of PAN-derived acetate anion with formic, glycolic or methoxyformic, and oxalic acid, respectively. It can thus be concluded that ion counts observed at the m/z associated with less abundant PANs were also biased high.

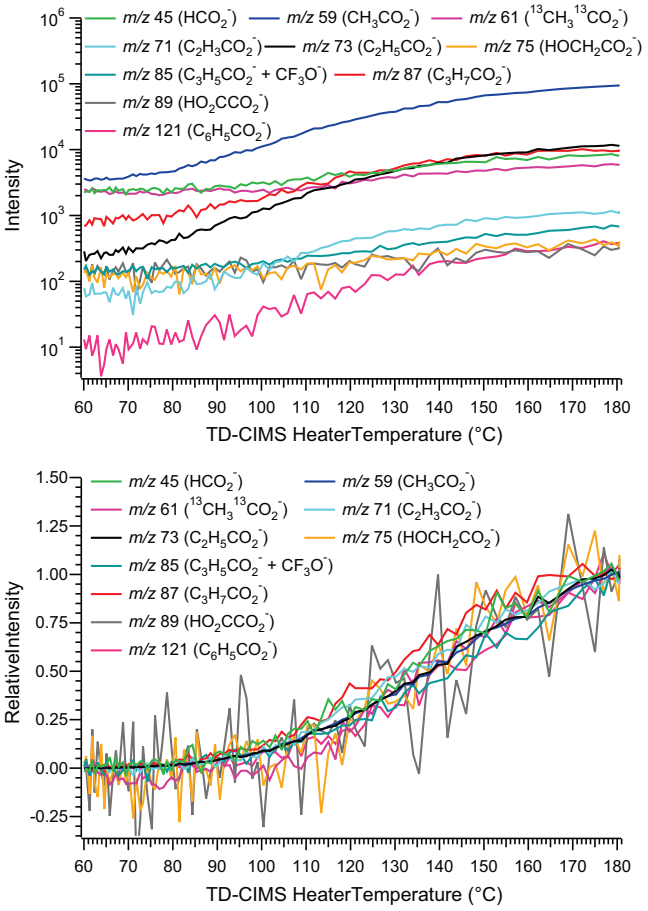

Fig. 7. Thermal dissociation profiles collected Calnex-LA. The top panel shows "raw" counts, and the bottom panel normalized counts. All masses monitored exhibit the same TD profile, even though they are known to differ considerably for the various PANs [31], suggesting that acetate generated from PAN in the inlet, rather than iodide anion was the major reagent ion contributing to ion counts at each of the masses.

4. Discussion

4.1. Thermal dissociation profiles and differences in PAN response factors

The TD-CIMS exhibits different sensitivities for different PANs, yet the similarity of NO_2 production in the TD-CRDS data suggests that the kinetics and activation barriers of reaction (1) are very similar for the various PANs. Since the anions generated are expected to be thermally stable, the differences in the TD-CIMS response factors are explained by differences in the decomposition rates of the peroxyacyl radicals generated in the inlet. This interpretation is consistent with the concentration independent TD profiles observed in this work. The data in Fig. 1 show losses of PA and PP radicals at TD-CIMS inlet temperatures above 190 °C, which suggests that a temperature dependent loss process also exists for the PA and PP radicals, but with higher activation barriers than for the MPA radical.

The temperature dependence of the TD-CIMS signals observed in this work is consistent with observations by Zheng et al. [31], who reported temperature-dependent responses for several PANs, including MPAN, APAN, CPAN ($H_3C–CH{=}CHC(O)O_2NO_2$), and PANs with more than 4 carbon atoms in a chain within the alkyl side group. Zheng et al. concluded that the thermal decomposition of the peroxyacyl radicals takes place in the CIMS inlet prior to their ionization, and noted that each of the larger PAN molecules has a distinct response curve as a function of inlet temperature [31]. The observed decomposition of the MPA radical also explains why the relative responses of TD-CIMS instruments to PAN and MPAN reported in the literature have been quite variable. For example, LaFranchi et al. reported a MPAN sensitivity of 1:4.3 relative to PAN [28], and Turnipseed et al. reported a relative sensitivity in the range of 1:3–1:10 (typically of 1:8) [30]. Our sensitivity to MPAN is lower (1:44 relative to PAN), which suggests that the shape of the TD profiles varies slightly between instruments depending on configuration and operating conditions.

The measurement of MPAN at m/z 85 is worrisome for reasons other than the TD-CIMS's low sensitivity. Zheng et al. noted that there is interference from CPAN, towards which the TD-CIMS is more sensitive [31]. Furthermore, there is a considerable background arising from CF_3O^- if Teflon tubing is used to construct the inlet. Even under environments where MPAN dominates the signal observed at m/z 85, the steep slope of the TD-profile at the normal inlet operating range of 180–190 °C will induce a loss of measurement accuracy as the sensitivity varies by a factor of 3 over a 10 degree temperature span. In addition, one would expect that noise is introduced at m/z 85 because it is challenging to maintain a constant inlet temperature in the field. Thus, the utility of TD-CIMS to accurately measure MPAN is limited, in particular in air masses of mixed biogenic and anthropogenic origin where crotonaldehyde and CPAN may be present [31].

4.2. Matrix effects

The TD-CIMS is clearly capable of quantifying PAN and PPN with exquisite sensitivity but the signals observed must be corrected for matrix effects. The customarily used ^{13}C-PAN internal standard can be used to correct for negative interference (i.e., loss of signal) due to the presence of NO, NO_2, and organic acids. However, the proton exchange reactions between acetate anion generated from PAN with other organic acids observed are of great concern, as they lead to positive interference at masses associated with the less abundant PANs. While proton exchange of acetate anion with acetic acid is of no further consequence, acetate anion will, in the majority of cases, proton-exchange with other organic acids, which tend to be stronger gas-phase acids [35]. Thus, this proton exchange chemistry generates artifact signals at masses associated with the less abundant PANs. While the internal standard can be used to correct for the loss of counts of the main ion (acetate), the internal standard cannot be used to correct for the artifact counts generated at the other masses. Such corrections would require knowledge of the ambient acid concentrations and a parameterization of the PAN dependent artifact signal for each mass monitored. In other words, the extent of this interference depends on the nature and the abundances of organic acids present in the sampled air, which are highly variable (e.g., [42]). In this work, we observed interference from organic acids at mixing ratios as low as 3 ppbv and PAN mixing ratios of about 2.2 ppbv (Fig. S-1A). This range of mixing ratios is expected to be easily achieved, if not exceeded, in only moderately polluted areas. We conclude that iodide ion TD-CIMS will generally overestimate concentrations of the less abundant PANs, in particular under polluted conditions (i.e., relatively high concentrations of PAN and organic acids).

An additional consequence of the proton exchange chemistry is the appearance of false "PAN-like" signals at masses for which no known PANs exist. Because titration with NO removes peroxyacyl radical which converts to acetate anion, addition of NO will also reduce the artifact signals, and thus does not serve as an accurate diagnostic to distinguish contributions of organic acids and PAN-type compounds to the signal observed at each mass. Of particular interest in this context is m/z 45 [35]. The PAN that would contribute to m/z 45 is peroxyformic nitric anhydride [43], which is unstable and not found in ambient air. Hence, this mass could potentially be

useful as semi-quantitative measure of the extent of interference from proton exchange with organic acids.

The TD profiles measured during Calnex-LA (Fig. 7) suggest that proton exchange with acetate anion was the dominant source of the ions observed at the masses associated with PANs less abundant than PAN and PPN (i.e., m/z 71, 87 and 121); if it had not been, the TD profiles would have resembled those recently reported by Zheng et al. [31]. On the other hand, the nearly identical TD profiles at m/z 45 and 89 and probably also at m/z 75 and 85 are "fake" PAN signals. We generally observed a signal at m/z 89 throughout Calnex-LA, but conclude that these counts are mainly due to proton exchange with oxalic acid.

The example shown in Fig. 7 is an extreme case since the counts at m/z 59 were 85,000, or 8.5% relative to the intended reagent ion, I^-. Since the overall rate law of the proton exchange reaction (5) is in all likelihood second order, one might think that the impact of interference from proton exchange can be lessened by dilution of the sampled air. However, this secondary inlet chemistry can be observed even when only very small concentrations (~100 pptv) of ^{13}C-PAN and approximately 8 ppbv of organic acid are present (e.g., Fig. 4, panels A and B). This implies that proton exchange can occur even when PAN abundances and overall ion counts are low. Under these conditions, it would be useful to keep the internal standard concentrations low as to not accelerate proton exchange chemistry.

The proton exchange chemistry was known prior to this work, as it has recently been taken advantage of to use acetate as the reagent ion for the detection of carboxylic acids and inorganic acids in the environment [35]. The extent of the acid interference will vary between instruments, as configurations and operating conditions (e.g., flow rates, voltages) are different, and there will be variability introduced from where the instruments are deployed (e.g., aircraft studies in remote regions vs. ground studies in polluted environments). Nevertheless, the carboxylic acid interference exists in all iodide ion TD-CIMS and needs to be considered even in regions with relatively small carboxylic acid abundances, as dissociation of PAN to produce acetate anions in the inlet suffices to produce an effect. Thus, iodide ion TD-CIMS users should exercise care in the interpretation of masses associated with the less abundant PANs.

5. Conclusion

This paper has described the application of TD-CIMS to measurements of PANs in ambient air. The TD-CIMS is clearly capable of quantifying PANs, PPN, etc. with exquisite sensitivity but the signals observed must be corrected for matrix effects arising from NO, NO_2 and organic acids. Some of these interferences can be tracked with ^{13}C-PAN internal standard, some cannot. In particular, the carboxylate anions generated in the IMR redistribute and deprotonate other organic acids present, which can result in a systematic positive interference for less abundant PANs. This effect can neither be remediated by dilution nor titration with NO. Thus, TD-CIMS will overestimate the abundances of the minor PANs, in particular in polluted environments. Furthermore, positive interference may arise from interference from peroxycarboxylic acids, which have been found in non-negligible concentrations in ambient air. Potential interference arising from peroxycarboxylic acids in iodide ion TD-CIMS are of concern and will need to be evaluated in further studies. Because of all these possible interferences, the TD-CIMS method cannot accurately measure the abundances of the less abundant PANs in polluted environments. A possible solution may be to equip the TD-CIMS inlet with a short preparatory-scale GC column to separate the PANs from each other (in particular from PAN) and from other interfering compounds. This could be accomplished without sacrificing high time resolution (since the column can be made very short) and without loss of sensitivity because the mass analyzer (operated in selected ion mode) can be synchronized to the column elution times.

Acknowledgements

The authors acknowledge funding from an Alberta Ingenuity Fund (AIF) New Faculty Award and from the National Science and Engineering Research Council of Canada (NSERC) in form of a Research Tools and Instruments (RTI) grant. HDO thanks John Nowak for useful discussions during the preparation of this manuscript.

Appendix A. Supplementary data

Supplementary data associated with this article can be found, in the online version, at doi:10.1016/j.ijms.2011.10.005.

References

[1] H.B. Singh, P.L. Hanst, Peroxyacetyl nitrate (PAN) in the unpolluted atmosphere—an important reservoir for nitrogen oxides, Geophys. Res. Lett. 8 (1981) 941–944.
[2] H.B. Singh, L.J. Salas, Peroxyacetyl nitrate in the free troposphere, Nature 302 (1983) 326–328.
[3] T. Nielsen, U. Samuelsson, P. Grennfelt, E.L. Thomsen, Peroxyacetyl nitrate in long-range transported polluted air, Nature 293 (1981) 553–555.
[4] S.A. Penkett, F.J. Sandalls, J.E. Lovelock, Observations of peroxyacetyl nitrate (PAN) in air in Southern England, Atmos. Environ. 9 (1975) 139–140.
[5] T.E. Kleindienst, Recent developments in the chemistry and biology of peroxyacetyl nitrate, Res. Chem. Intermed. 20 (1994) 335–384.
[6] B. Chuong, P. Stevens, Measurements of the kinetics of the OH-initiated oxidation of methyl vinyl ketone and methacrolein, Int. J. Chem. Kinet. 36 (2004) 12–25.
[7] J. Williams, J.M. Roberts, F.C. Fehsenfeld, S.B. Bertman, M.P. Buhr, P.D. Goldan, G. Hubler, W.C. Kuster, T.B. Ryerson, M. Trainer, V. Young, Regional ozone from biogenic hydrocarbons deduced from airborne measurements of PAN, PPN, and MPAN, Geophys. Res. Lett. 24 (1997) 1099–1102.
[8] J.M. Roberts, J. Williams, K. Baumann, M.P. Buhr, P.D. Goldan, J. Holloway, G. Hubler, W.C. Kuster, S.A. McKeen, T.B. Ryerson, M. Trainer, E.J. Williams, F.C. Fehsenfeld, S.B. Bertman, G. Nouaime, C. Seaver, G. Grodzinsky, M. Rodgers, V.L. Young, Measurements of PAN, PPN, and MPAN made during the 1994 and 1995 Nashville Intensives of the Southern Oxidant Study: implications for regional ozone production from biogenic hydrocarbons, J. Geophys. Res.: Atmos. 103 (1998) 22473–22490.
[9] R.K. Talukdar, J.B. Burkholder, A.M. Schmoltner, J.M. Roberts, R.R. Wilson, A.R. Ravishankara, Investigation of the loss processess for peroxyacetyl nitrate in the atmosphere—UV photolysis and reaction with OH, J. Geophys. Res.: Atmos. 100 (1995) 14163–14173.
[10] L. Zhang, D.J. Jacob, K.F. Boersma, D.A. Jaffe, J.R. Olson, K.W. Bowman, J.R. Worden, A.M. Thompson, M.A. Avery, R.C. Cohen, J.E. Dibb, F.M. Flock, H.E. Fuelberg, L.G. Huey, W.W. McMillan, H.B. Singh, A.J. Weinheimer, Transpacific transport of ozone pollution and the effect of recent Asian emission increases on air quality in North America: an integrated analysis using satellite, aircraft, ozonesonde, and surface observations, Atmos. Chem. Phys. 8 (2008) 6117–6136.
[11] R.A. Kotchenruther, D.A. Jaffe, H.J. Beine, T.L. Anderson, J.W. Bottenheim, J.M. Harris, D.R. Blake, R. Schmitt, Observations of ozone and related species in the northeast Pacific during the PHOBEA campaigns 2. Airborne observations, J. Geophys. Res.: Atmos. 106 (2001) 7463–7483.
[12] E.V. Fischer, D.A. Jaffe, D.R. Reidmiller, L. Jaegle, Meteorological controls on observed peroxyacetyl nitrate at Mount Bachelor during the spring of 2008, J. Geophys. Res.: Atmos. 115 (2010) D03302, doi:03310.01029/02009JD012776.
[13] W.J. Moxim, H. Levy, P.S. Kasibhatla, Simulated global tropospheric PAN: its transport and impact on NO_x, J. Geophys. Res.: Atmos. 101 (1996) 12621–12638.
[14] R.C. Hudman, D.J. Jacob, O.R. Cooper, M.J. Evans, C.L. Heald, R.J. Park, F. Fehsenfeld, F. Flocke, J. Holloway, G. Hubler, K. Kita, M. Koike, Y. Kondo, A. Neuman, J. Nowak, S. Oltmans, D. Parrish, J.M. Roberts, T. Ryerson, Ozone production in transpacific Asian pollution plumes and implications for ozone air quality in California, J. Geophys. Res.: Atmos. 109 (2004).
[15] M.J. Alvarado, J.A. Logan, J. Mao, E. Apel, D. Riemer, D. Blake, R.C. Cohen, K.E. Min, A.E. Perring, E.C. Browne, P.J. Wooldridge, G.S. Diskin, G.W. Sachse, H. Fuelberg, W.R. Sessions, D.L. Harrigan, G. Huey, J. Liao, A. Case-Hanks, J.L. Jimenez, M.J. Cubison, S.A. Vay, A.J. Weinheimer, D.J. Knapp, D.D. Montzka, F.M. Flocke, I.B. Pollack, P.O. Wennberg, A. Kurten, J. Crounse, J.M.S. Clair, A. Wisthaler, T. Mikoviny, R.M. Yantosca, C.C. Carouge, P. Le Sager, Nitrogen oxides and PAN in plumes from boreal fires during ARCTAS-B and their impact on ozone: an integrated analysis of aircraft and satellite observations, Atmos. Chem. Phys. 10 (2010) 9739–9760.

[16] J.M. Roberts, PAN related compounds, in: R. Koppmann (Ed.), Volatile Organic Compounds in the Atmosphere, Blackwell Publishing, Oxford, UK, 2007, pp. 221–268.
[17] F.M. Flocke, A.J. Weinheimer, A.L. Swanson, J.M. Roberts, R. Schmitt, S. Shertz, On the measurement of PANs by gas chromatography and electron capture detection, J. Atmos. Chem. 52 (2005) 19–43.
[18] P. Blanchard, P.B. Shepson, K.W. So, H.I. Schiff, J.W. Bottenheim, A.J. Gallant, J.W. Drummond, P. Wong, A comparison of calibration and measurement techniques for gas chromatographic determination of atmospheric peroxyacetyl nitrate (PAN), Atmos. Environ. A 24 (1990) 2839–2846.
[19] P. Blanchard, P.B. Shepson, H.I. Schiff, J.W. Drummond, Development of a gas-chromatograph for trace-level measurement of peroxyacetyl nitrate using chemical amplification, Anal. Chem. 65 (1993) 2472–2477.
[20] D.A. Day, P.J. Wooldridge, M.B. Dillon, J.A. Thornton, R.C. Cohen, A thermal dissociation laser-induced fluorescence instrument for in situ detection of NO_2, peroxy nitrates, alkyl nitrates, and HNO_3, J. Geophys. Res.: Atmos. 107 (2002) 4046, D6, doi:4010.1029/2001JD000779.
[21] P.J. Wooldridge, A.E. Perring, T.H. Bertram, F.M. Flocke, J.M. Roberts, H.B. Singh, L.G. Huey, J.A. Thornton, G.M. Wolfe, J.G. Murphy, J.L. Fry, A.W. Rollins, B.W. LaFranchi, R.C. Cohen, Total peroxy nitrates (ΣPNs) in the atmosphere: the Thermal Dissociation-Laser Induced Fluorescence (TD-LIF) technique and comparisons to speciated PAN measurements, Atmos. Meas. Technol. 3 (2010) 593–607.
[22] D. Paul, A. Furgeson, H.D. Osthoff, Measurement of total alkyl and peroxy nitrates by thermal decomposition cavity ring-down spectroscopy, Rev. Sci. Instrum. 80 (2009) 114101, doi:114110.111063/114101.3258204.
[23] D. Paul, H.D. Osthoff, Absolute measurements of total peroxy nitrate mixing ratios by thermal dissociation blue diode laser cavity ring-down spectroscopy, Anal. Chem. 82 (2010) 6695–6703.
[24] A. Hansel, A. Wisthaler, A method for real-time detection of PAN, PPN and MPAN in ambient air, Geophys. Res. Lett. 27 (2000) 895–898.
[25] R. Holzinger, J. Williams, G. Salisbury, T. Klupfel, M. de Reus, M. Traub, P.J. Crutzen, J. Lelieveld, Oxygenated compounds in aged biomass burning plumes over the Eastern Mediterranean: evidence for strong secondary production of methanol and acetone, Atmos. Chem. Phys. 5 (2005) 39–46.
[26] D.R. Hastie, J. Gray, V.S. Langford, R. Maclagan, D.B. Milligan, M.J. McEwan, Real-time measurement of peroxyacetyl nitrate using selected ion flow tube mass spectrometry, Rapid Commun. Mass Spectr. 24 (2010) 343–348.
[27] D.L. Slusher, L.G. Huey, D.J. Tanner, F.M. Flocke, J.M. Roberts, A thermal dissociation-chemical ionization mass spectrometry (TD-CIMS) technique for the simultaneous measurement of peroxyacyl nitrates and dinitrogen pentoxide, J. Geophys. Res.: Atmos. 109 (2004) D19315, doi:19310.11029/12004JD004670.
[28] B.W. LaFranchi, G.M. Wolfe, J.A. Thornton, S.A. Harrold, E.C. Browne, K.E. Min, P.J. Wooldridge, J.B. Gilman, W.C. Kuster, P.D. Goldan, J.A. de Gouw, M. McKay, A.H. Goldstein, X. Ren, J. Mao, R.C. Cohen, Closing the peroxy acetyl nitrate budget: observations of acyl peroxy nitrates (PAN, PPN, and MPAN) during BEARPEX 2007, Atmos. Chem. Phys. 9 (2009) 7623–7641.
[29] G.M. Wolfe, J.A. Thornton, V.F. McNeill, D.A. Jaffe, D. Reidmiller, D. Chand, J. Smith, P. Swartzendruber, F. Flocke, W. Zheng, Influence of trans-Pacific pollution transport on acyl peroxy nitrate abundances and speciation at Mount Bachelor Observatory during INTEX-B, Atmos. Chem. Phys. 7 (2007) 5309–5325.
[30] A.A. Turnipseed, L.G. Huey, E. Nemitz, R. Stickel, J. Higgs, D.J. Tanner, D.L. Slusher, J.P. Sparks, F. Flocke, A. Guenther, Eddy covariance fluxes of peroxyacetyl nitrates (PANs) and NOy to a coniferous forest, J. Geophys. Res.: Atmos. 111 (2006) D09304, doi:09310.01029/02005JD006631.
[31] W. Zheng, F.M. Flocke, G.S. Tyndall, A. Swanson, J.J. Orlando, J.M. Roberts, L.G. Huey, D.J. Tanner, Characterization of a thermal decomposition chemical ionization mass spectrometer for the measurement of peroxy acyl nitrates (PANs) in the atmosphere, Atmos. Chem. Phys. Discuss. 11 (2011) 8461–8513.
[32] A. Roiger, H. Aufmhoff, P. Stock, F. Arnold, H. Schlager, An aircraft-borne chemical ionization ion trap mass spectrometer (CI-ITMS) for fast PAN and PPN measurements, Atmos. Meas. Technol. 4 (2011) 173–188.
[33] G.M. Wolfe, J.A. Thornton, R.L.N. Yatavelli, M. McKay, A.H. Goldstein, B. LaFranchi, K.E. Min, R.C. Cohen, Eddy covariance fluxes of acyl peroxy nitrates (PAN, PPN and MPAN) above a Ponderosa pine forest, Atmos. Chem. Phys. 9 (2009) 615–634.
[34] A. Furgeson, L.H. Mielke, D. Paul, H.D. Osthoff, A photochemical source of peroxypropionic and peroxyisobutanoic nitric anhydride, Atmos. Environ. 45 (2011) 5025–5032.
[35] P. Veres, J.M. Roberts, C. Warneke, D. Welsh-Bon, M. Zahniser, S. Herndon, R. Fall, J. de Gouw, Development of negative-ion proton-transfer chemical-ionization mass spectrometry (NI-PT-CIMS) for the measurement of gas-phase organic acids in the atmosphere, Int. J. Mass Spectr. 274 (2008) 48–55.
[36] J.M. Roberts, P. Veres, C. Warneke, J.A. Neuman, R.A. Washenfelder, S.S. Brown, M. Baasandorj, J.B. Burkholder, I.R. Burling, T.J. Johnson, R.J. Yokelson, J. de Gouw, Measurement of HONO, HNCO, and other inorganic acids by negative-ion proton-transfer chemical-ionization mass spectrometry (NI-PT-CIMS): application to biomass burning emissions, Atmos. Meas. Technol. 3 (2010) 981–990.
[37] X. Zhang, Z.M. Chen, S.Z. He, W. Hua, Y. Zhao, J.L. Li, Peroxyacetic acid in urban and rural atmosphere: concentration, feedback on PAN-NO_x cycle and implication on radical chemistry, Atmos. Chem. Phys. 10 (2010) 737–748.
[38] L.H. Mielke, A. Furgeson, H.D. Osthoff, Observation of ClNO2 in a mid-continental urban environment, Environ. Sci. Technol. 45 (2011) 8889–8896.
[39] T. Nielsen, A.M. Hansen, E.L. Thomsen, A convenient method for preparation of pure standards of peroxyacetyl nitrate for atmospheric analyses, Atmos. Environ. 16 (1982) 2447–2450.
[40] J.S. Gaffney, R. Fajer, G.I. Senum, An improved procedure for high-purity gaseous peroxyacyl nitrate production—use of heavy lipid solvents, Atmos. Environ. 18 (1984) 215–218.
[41] J. Sehested, L.K. Christensen, T. Mogelberg, O.J. Nielsen, T.J. Wallington, A. Guschin, J.J. Orlando, G.S. Tyndall, Absolute and relative rate constants for the reactions $CH_3C(O)O_2 + NO$ and $CH_3C(O)O_2 + NO_2$ and thermal stability of $CH_3C(O)O_2NO_2$, J. Phys. Chem. A 102 (1998) 1779–1789.
[42] J. Lawrence, P. Koutrakis, Measurement and speciation of gas and particulate phase organic acidity in an urban environment 2. Speciation, J. Geophys. Res. 101 (1996) 9171–9184.
[43] B.W. Gay, R.C. Noonan, J.J. Bufalini, P.L. Hanst, Photochemical synthesis of peroxyacyl nitrates in gas phase via chlorine-aldehyde reaction, Environ. Sci. Technol. 10 (1976) 82–85.